16th World Conference on Earthquake, 16WCEE 2017
Santiago Chile, January 9th to 13th 2017
Paper N° 59 (Abstract ID)
Registration Code: S-T1459979109

DEFORMATION CAPACITY OF SHEAR PANEL STEEL DAMPER AND ITS REFLECTION TO AIJ FATIGUE DESIGN REQUIREMENTS

H. Tamai[(1)] and K. Kasai[(2)]

[(1)] *Professor, Structural Engineering Division, Faculty of Engineering, Nagasaki Univ., Japan, tamix@nagasaki-u.ac.jp*
[(2)] *Professor and Director, Structural Engineering Research Center, Tokyo Institute of Technology, Japan, e-mail address*
…

Abstract

Shear panel dampers consisting of stiffeners and panels surrounded by four flanges are used as aseismic hysteretic dampers for buildings in Japan. Cracks can form easily in a shear panel damper when shear buckling occurs during the cyclic loading caused by a severe earthquake. For a relatively thin panel with a large width-to-thickness ratio, the damper's plastic deformation capacity and the presence of shear buckling can be evaluated from the maximum deformation angle. However, when it is relatively small, very-low-cycle fatigue life for a relatively thick panel must be known to predict the usage limit of the damper, because the failure pattern changes when cracks form in the weld between the panels and flanges. Fatigue life relations for a thick shear panel damper with parameters of normalized width-to-thickness ratio and deformation angle are presented. A method for predicting the fatigue life under severe earthquake conditions is also presented. To validate the prediction expression, cyclic loading tests were performed on a shear panel damper and reviewed. The applicability of the method for predicting the fatigue life was confirmed through non-stationary cyclic loading tests. These results showed the validity and effectiveness of the expressions and the method.

Keywords: damage factor; shear panel; plastic deformation capacity; fatigue toughness; AIJ design requirements

1. Introduction

Steel shear panel dampers (S.P.Ds) consisting of stiffeners and a panel surrounded by four flanges, resembling North American shear links, are used as aseismic hysteretic dampers for buildings in Japan (Fig. 1). S.P.Ds are not subjected to axial forces and are designed for inclusion in seismic damping systems applied to buildings. Loading tests on long and short links in eccentrically braced frames have been performed by many researchers, including [1]-[5]). A buckling prediction expression for shear links was proposed by Kasai and Popov [4]. Design codes such as the IBC[6] in North America adopted this buckling prediction for panels in shear links. Steel dampers are designed to maintain a damping function until the building reaches the designed deformation amplitude under seismic loading. Hence, the usage limit of a steel S.P.D. is defined as the ultimate deformation capacity permitting maintenance of the damper function. The ultimate deformation capacity can be classified by both monotonic and cyclic deformation. To evaluate the monotonic deformation capacity, design considerations and the interactions between the damper and structural members are required to estimate the rupture and buckling of a damper. For the cyclic deformation capacity, design considerations are required to estimate the fatigue toughness and stable restoring force characteristics of the damper. The deformation capacity under cyclic deformation is typically measured by the ductility factor, cumulative ductility factor, and absorbing energy for seismic loading, when the number of cycles is relatively small.

The damage factor is based on very-low-cycle fatigue test results. Other indices, such as the cumulative ductility factor, are used in designs using the earthquake response. The cumulative ductility factor is the summation of the absolute plastic deformation increments divided by the elastic limit deformation. The earthquake response comprises cyclic loading with small and large deformation amplitudes. Loading with a larger deformation amplitude should cause more damage than the magnification of the deformation amplitude [7],[8]. Because the cumulative ductility factor is proportional to the deformation amplitude, the damage characteristics cannot be represented by the cumulative ductility factor. However, the damage factor can account for the damage characteristics by summing the damage corresponding to the deformation amplitude. Hence, it is possible to judge whether a damper has reached its usage limit based on the damage factors corresponding to the deformation amplitude under severe earthquakes [9],[10][11]. The damage factor is used as the performance index of the fatigue toughness of a damper for strong wind loading, in which the number of loading cycles is very large compared to that for earthquake loading[12]. Hence, we focused here on the damage factor as a usage limit index. When the factor reaches unity, fracture occurs. Details of the damage index are described in section 4.1. Cracks can easily form in an S.P.D. experiencing excessive shear buckling during the cyclic loading caused by a severe earthquake. Shear buckling and the plastic deformation capacity of a panel damper can be detected by checking the maximum deformation angle. For a relatively thin panel, when the width-to-thickness ratio is large, the plastic deformation capacity can be evaluated from the maximum deformation angle.

The usage limit of the S.P.D. from shear buckling can be evaluated by the equivalent shear buckling deformation angle [4],[13]. However, when the width-to-thickness ratio is relatively small, as for relatively thick panels, very-low-cycle fatigue life data is essential to predict the damper's usage limit because the failure pattern changes when cracks form in the welds between panel and flanges.

In this study, we adopted the very-low-cycle fatigue relation as a performance expression of the damper. The very-low-cycle fatigue relation correlates the number of loading cycles to the fracture and deformation angles of the damper. The very-low-cycle fatigue relation is presented for a thick S.P.D. with parameters such as normalized width-to-thickness ratio of the panel and deformation angle. The fatigue life of a damper under constant amplitude loading has been reviewed in domestic and foreign reports on both non-stiffened and stiffened shear panels. We demonstrated the applicability of the fatigue relation in both non-stiffened and stiffened shear panels. Finally, a method for predicting fatigue life under severe earthquake conditions is presented. This method includes a very-low-cycle fatigue relation and a cumulative damage rule. It was validated by a non-stationary loading test. The obtained results were reflected in the AIJ design requirements "The Recommended Provision for Seismic Damping Systems Applied to Steel Structures (2014)[14]."

2. Very-Low-Cycle Fatigue Relation

2.1 Un-stiffened Shear Panel

This section first presents the fatigue relation for calculating the damage factor of an S.P.D. The Manson-Coffin fatigue relation is satisfactory for predicting the fatigue life of metal materials. The fatigue relation correlates plastic strain to the number of cycles at break [7]. The critical usage limit of a damper is defined as the point at which the strength of an S.P.D. decreases to 0.90 of the maximum strength. Tamai et al. [10] showed that the fatigue life of an S.P.D. is well described by Manson-Coffin type fatigue relations by setting the plastic shear deformation angle as the argument of the relation. For an S.P.D., the following equation describes the case in which the panel is relatively thick and does not undergo shear buckling.

$$N_f = \frac{1}{2} \cdot \left| \frac{\gamma_a^{(p)}}{\gamma_f} \right|^{-C} \tag{1}$$

N_f is the number of half-cycles after which the load amplitude decreases to 0.9 of the maximum value under single-level loading with constant shear displacement amplitude. C and γ_f are experimental constants. $\gamma_a^{(p)}$ is derived from the following equation:

$$\gamma_a^{(p)} = \gamma_a - \frac{Q_a}{Q_p} \cdot \gamma_p \tag{2}$$

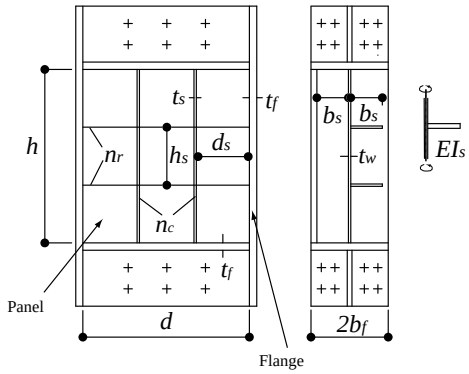

Fig. 1 – Dimensions of Representative S.P.D.

where γ_a, Q_a, γ_p, and Q_p are the shear deformation angle amplitude, loading amplitude, elastic limit deformation angle, and elastic limit load of the S.P.D. γ_f physically corresponds to the ultimate plastic deformation angle capacity, because Eq. (1) is satisfied when $\gamma_a^{(p)}$ is equal to γ_f under monotonic loading ($N_f = 1/2$). The dimensions of a representative S.P.D. are shown in Fig. 1. Narihara and Nakagomi [15] adopted a modification of Eq. (1) for practical use. They used γ_a in place of $\gamma_a^{(p)}$ in Eq. (1) and a new panel width-to-thickness ratio, with a buckling coefficient for a rectangular subpanel:

$$\frac{h'}{t_w} = \frac{h_s}{t_w} \cdot \sqrt{\frac{9.34}{5.34 + 4.00/\left(d_s/h_s\right)^2}} \tag{3.a}$$

where d_s, h_s, and t_w are the subpanel width, height, and thickness. To accommodate the subpanel steel grade and aspect ratio, the normalized panel width-to-thickness ratio providing the maximum shear strength τ_u and the buckling coefficient for a simply supported rectangular plate κ_s are defined. The test results of S.P.D. for various steel grades are analyzed using the normalized panel width-to-thickness ratio.

$$\frac{h''}{t_w} = \frac{h_s}{t_w} \cdot \sqrt{\frac{\tau_u}{\kappa_s \cdot E}} \tag{3.b}$$

where E is the Young's modulus of the steel.

$$\kappa_s = 5.34 + 4.00/\left(\frac{d_s}{h_s}\right)^2 \text{ for } \frac{d_s}{h_s} \geq 1 \quad , \quad \kappa_s = 4.00 + 5.34/\left(\frac{d_s}{h_s}\right)^2 \text{ for } \frac{d_s}{h_s} < 1 \tag{4.a,b}$$

Because a damper is subjected to large cyclic deformations in severe earthquakes, the maximum shear strength was adopted in Eq. (3.b). The fatigue relations between the shear deformation angle γ_a and the fatigue life N_f within various ranges of the normalized width-to-thickness ratio were derived from tests by a least-square method.

$$N_f = \frac{1}{2} \cdot \left| \frac{\gamma_a}{\gamma_f} \right|^{-C} \tag{5.a}$$

Data from previously published papers were investigated to show the applicability of the fatigue relation expressed in Eq. (5.a). Koga et al. [11], Sekine et al. [16], Takenaka et al. [17], Tagami et al. [18], Kondou et al. [19], Kanazawa et al. [20], Koga [21], and Hanai et al. [22] performed single-level loading tests for a square panel without stiffener. The steel grades of the panels were LY100, LY225, LY235, and SN400. The variables C and γ_f in Eq. (5.a) were derived from test data within various ranges of the normalized panel width-to-thickness ratio $h_s / t_w \cdot \sqrt{\tau_u / (\kappa_s \cdot E)}$ by means of a least-square method.

$$\gamma_f = 0.482, C = 2.40, R = -0.980 \text{ for } 0.150 \le \frac{h_s}{t_w} \cdot \sqrt{\frac{\tau_u}{\kappa_s \cdot E}} \le 0.165$$

$$\gamma_f = 0.410, C = 2.27, R = -0.986 \text{ for } 0.299 \le \frac{h_s}{t_w} \cdot \sqrt{\frac{\tau_u}{\kappa_s \cdot E}} \le 0.303$$

$$\gamma_f = 0.365, C = 2.17, R = -0.998 \text{ for } 0.339 \le \frac{h_s}{t_w} \cdot \sqrt{\frac{\tau_u}{\kappa_s \cdot E}} \le 0.355$$

$$\gamma_f = 0.252, C = 1.94, R = -0.978 \text{ for } 0.500 \le \frac{h_s}{t_w} \cdot \sqrt{\frac{\tau_u}{\kappa_s \cdot E}} \le 0.505$$

$$\gamma_f = 0.273, C = 1.52, R = -0.977 \text{ for } 0.655 \le \frac{h_s}{t_w} \cdot \sqrt{\frac{\tau_u}{\kappa_s \cdot E}} \le 0.707$$

(5.b-f)

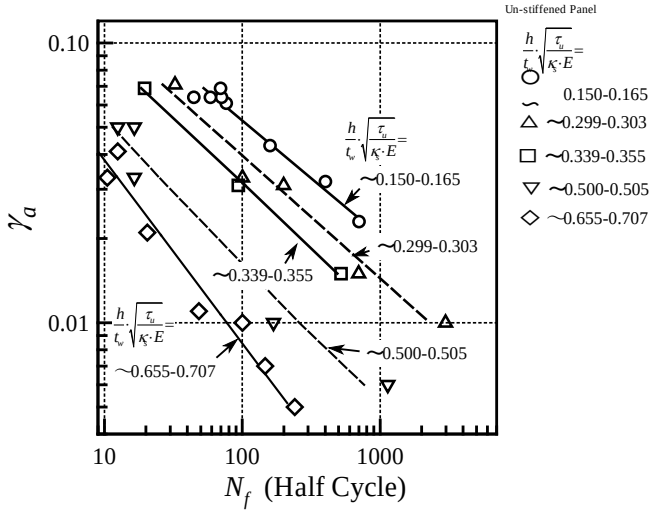

Fig. 2 – Fatigue Relation of Un-Stiffened S.P.D.

N_f for $h_s / t_w \cdot \sqrt{\tau_u / (\kappa_s \cdot E)} = 0.707$, 0.505, and 0.303 counts the number of cycles after which the load amplitude is degraded to 0.95 of the maximum loading amplitude. The data of the shaded rows in Table 1 are not used because the loading conditions differ from those used to obtain the other data. The loading speeds of the test are middle- and high-strain-rate dynamic loading. R is a correlation coefficient. The fatigue relation data within various ranges of normalized panel width-to-thickness ratio correlates closely with results from Eq. (5.a). When the normalized panel width-to-thickness ratio exceeds 0.50, R approaches -1.0 with values such as -0.978 and -0.977, as the variance of Eq. (5.a) increases. Fig. 2 shows the relationship between γ_a and N_f. The variance of the fatigue relation is affected by shear buckling. Fig. 3 shows the relationship between the experimental coefficients C and γ_f, and the normalized panel width-to-thickness ratio $h_s / t_w \cdot \sqrt{\tau_u / (\kappa_s \cdot E)}$ as indicated with white circles and triangles. Regression lines are shown as straight solid lines in Fig. 3. The ultimate plastic deformation angle γ_f and the gradient of fatigue relation C varies linearly in a double-logarithmic diagram with normalized panel width-to-thickness ratios between 0.15 and 0.70. This indicates that the fatigue lifetimes of different failure modes, such as weld cracks and shear buckling, can be represented by the same equation. The regression lines derived from Eqs. (5.b-f) are shown as follows:

$$C = -1.72 \cdot \frac{h_s}{t_w} \cdot \sqrt{\frac{\tau_u}{\kappa_s \cdot E}} + 2.74, \quad R = -0.981 \quad , \quad \gamma_f = -0.449 \cdot \frac{h_s}{t_w} \cdot \sqrt{\frac{\tau_u}{\kappa_s \cdot E}} + 0.534, \quad R = -0.925 \tag{6.a,b}$$

2.2 Stiffened Shear Panel

The damper's plastic deformation capacity can be enhanced by installing vertical and horizontal stiffeners on the panel. This section investigates the applicability of the fatigue relation for such stiffened shear panels. Reports describing single-level loading tests on stiffened shear panel were reviewed, including Takenaka et al. [17], Izumi et al. [23],[24], Ryujin et al. [25], Ueki et al. [26], Fujinami, et al. [27], Tukatani et al. [28], Kanazawa et al. [29], and Ida et al. [30].

The amplitude of the effective deformation angle γ_a^* was derived as follows:

$$\gamma_a^* = \frac{h}{(h-2\cdot n_r\cdot t_s)}\cdot\gamma_a \ , \ h_s=(h-n_r\cdot t_s)/(n_r+1)\,, \ d_s=(d-n_c\cdot t_s)/(n_c+1) \qquad (7.a,b,c)$$

where n_r and n_c are the number of stiffeners in the width and height directions, respectively, of the panel. The flexural rigidity ratio and optimum ratio for the stiffener γ_s and γ_s^* are defined as follows.

$$\gamma_s = \frac{E\cdot I_s}{D\cdot h} \qquad (8.a)$$

for $n_r = n_c = n$

$$\gamma_s^* = \left(\frac{23.1}{n^{2.5}}-\frac{1.35}{n^{0.5}}\right)\cdot\frac{\left(1+\alpha^{\frac{3}{n}-0.3}\right)^{2n-1}}{1+\alpha^{5.3-0.6n-\frac{3}{n}}} \qquad (8.b)$$

for $n_r = n$ and $n_c = 0$

$$\gamma_s^* = \frac{27.3\cdot n^{0.6}\cdot\alpha-23.3\cdot\alpha}{0.20\cdot n^{0.7}-0.60/\alpha+0.52/\alpha^2} \qquad (8.c)$$

where α is the panel aspect ratio.

$$\alpha = \frac{d}{h} \quad (0.5\le\alpha\le 2.0) \qquad (8.d)$$

D is the plate flexural rigidity of the panel.

$$D = \frac{E\cdot t_w^3}{12\cdot(1-\nu^2)} \qquad (8.e)$$

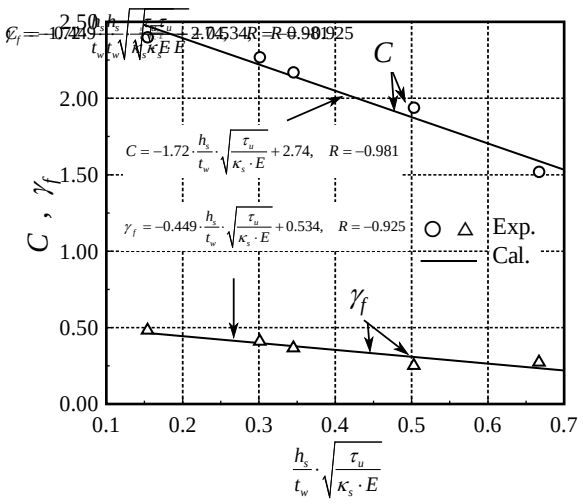

Fig. 3 – Relation between Experimental Coefficient and Normalized Panel Width-to-Thickness Ratio

$E\cdot I_s$ is the flexural rigidity of the stiffener, while n is the total number of stiffeners in the width and height directions.

The optimum stiffener flexural rigidity ratio is defined as a sectional property of the stiffener, in which the subpanels undergo shear buckling before the panel does [31]. Fig. 4 shows the relationship between the shear deformation angle amplitude γ_a and the fatigue life N_f. Experimental results for the un-stiffened panel are displayed as white symbols and those for stiffened panels are shown as black painted symbols, classified by the various ranges of the normalized panel width-to-thickness ratio. The fatigue relation lines calculated from Eq. (5.a), and Eqs. (6.a,b) with $h_s/t_w\cdot\sqrt{\tau_u/(\kappa_s\cdot E)}$ = 0.15, 0.2, 0.3, 0.4, 0.5, 0.6, and 0.7 are also shown in Fig. 4. The data of the stiffened panel use the effective deformation amplitude γ_a^* instead of γ_a.

Fig. 5 shows the same relationship as that in Fig. 4. Failure modes in which cracks are initiated in the center of the panel are shown as white symbols while those in which cracks grow in the welds of the panel with the flanges are shown as black painted symbols. The data are further classified by panel steel grade.

The symbols (Fig. ●, (△,▲) 4 show the panel steel grades of LY100, LY235, and SN400, respectively, as assigned by JIS (Japan Industrial Standards).

From these results, the following remarks are made. The fatigue life of a stiffened shear panel is slightly shorter than that of an un-stiffened panel when the subpanel width-to-thickness ratio is below 0.339. The same fatigue relationships (Eq. (5.a), Eqs. (6.a,b)) can be used to describe a stiffened panel when the subpanel width-to-thickness ratio is lower than 0.339. From Fig. 5, when γ_a exceeds 0.6 radians and the normalized panel width-to-thickness ratio is below 0.25, cracks grow in the weld between the panel and the flanges. When γ_a is below 0.10 radians and the normalized subpanel width-to-thickness ratio exceeds 0.30, cracks form in the center of the panel.

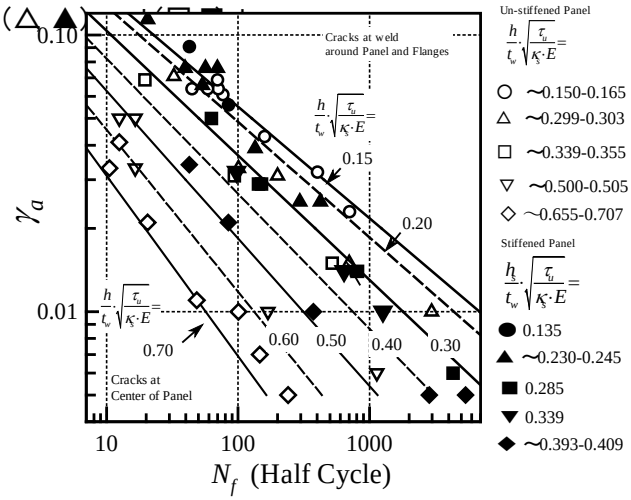

Fig. 4 – Influence of Panel Stiffeners on Fatigue Life

3. Comparison of Failure Mode and Shear Buckling under Single-level Loading

The fatigue relationship obtained in the previous section is applicable to panels of various steel grades and width-to-thickness ratios. For a relatively thick panel, cracks grow in the weld around the panel and flanges. For a relatively thin panel, cracks grow in the center of the panel, and large out-of-plane deflections due to shear buckling are observed. The restoring force characteristics of the panel are not spindle-shaped because the load stiffness has a negative relationship with displacement. The shear buckling of the panel reduces the fatigue life under single-level cyclic loading. Therefore, there is an applicable limit to the width-to-thickness ratio for the fatigue relationship. This section discusses the applicable limit by comparing the failure modes of the test results and shear buckling prediction zones by using the equivalent shear buckling deformation angle [4],[13].

The amplitude of the shear buckling deformation angle of the panel is shown as follows.

$$\gamma_a = \frac{1}{2}\left(\frac{\overline{\gamma}_B}{\gamma_y}+1\right)\cdot\gamma_y \qquad (9)$$

where

$$\frac{\overline{\gamma}_B}{\gamma_y} = A\cdot\frac{\pi^2}{12\cdot(1-\nu^2)}\cdot\frac{1}{\left(\frac{h_s}{t_w}\cdot\sqrt{\frac{\tau_y}{\kappa_c\cdot E}}\right)^2} \qquad (10.a)$$

$$\kappa_c = 8.98+5.60/\left(\frac{d_s}{h_s}\right)^2 \quad \text{for } \frac{d_s}{h_s}\geq 1 \qquad (10.b)$$

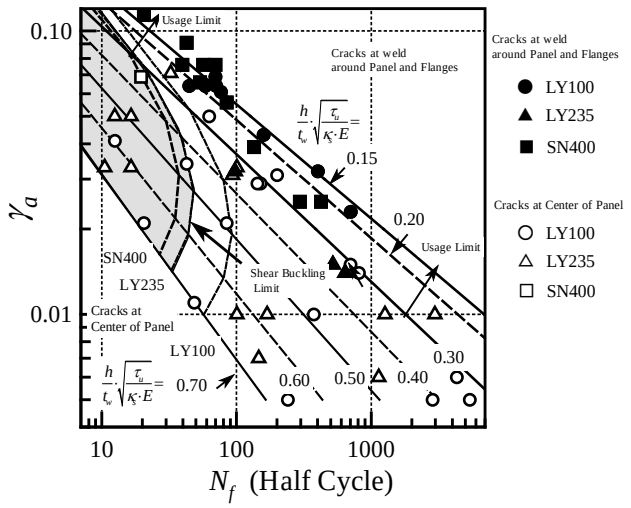

Fig. 5 – Comparison of Failure Mode and Shear Buckling Zone

$$\kappa_c = 5.60 + 8.98 / \left(\frac{d_s}{h_s} \right)^2 \quad \text{for } \frac{d_s}{h_s} < 1 \qquad (10.c)$$

γ_y and τ_y denote the yield shear deformation angle and the yield shear stress, respectively, and A is an experimental constant equal to 3.65.

The procedures for drawing a shear buckling prediction line in the fatigue relation diagram, Fig. 5, are presented as follows.

1) We select the steel grade of the panel, e.g., LY100, LY235, or SN400. The yield stresses and tensile strengths are 100 and 250 N/mm^2, 235 and 350 N/mm^2, and 259 and 400 N/mm^2, respectively.
2) We specify the normalized panel width-to-thickness ratio.
3) We derive the shear buckling deformation angle γ_a from Eq. (9), assuming that the aspect ratio of panel is 1.0.
4) By substituting the normalized panel width-to-thickness ratio into Eqs. (6.a,b), we derive the experimental constants C and γ_f.
5) We derive the fatigue life N_f from Eq. (5.a) with C and γ_f. Hence, the relation between γ_a and N_f can be plotted in the fatigue relation diagram.
6) By repeating procedures 2) to 5), the shear buckling limit line can be drawn in the fatigue relation diagram.

The shear buckling limits are shown as broken lines for square panels of steel grades SN400, LY235, and LY100 in Fig. 5. The shaded area in Fig. 5 shows the shear buckling zone for an LY235-grade steel panel. From these results, the following remarks can be made. When the normalized panel width-to-thickness ratio is below 0.25, cracks grow in the weld between the panel and flanges or in that between the flanges and end plate, without strength degradation by shear buckling, even if the deformation angle amplitude exceeds 0.06 radians. However, when the normalized panel width-to-thickness ratio exceeds 0.30, cracks grow at the center of the panel. The joints between panel and flange and between flanges and endplate are fillet and butt welds, respectively. The size of the weld is equal to the thickness of the thinner plate. Because the fatigue life increases when the shear deformation angle of the panel γ_a is below 0.01 radians, cracks can grow in the center of the panel even if the normalized panel width-to-thickness ratio is below 0.30. The obtained results are summarized as follows.

1) The fatigue relation sufficiently describes the behavior of the stiffened panel with a normalized panel width-to-thickness ratio below 0.339.
2) When the normalized width-to-thickness ratio is below 0.30, indicating a relatively thick panel, cracks grow around the welds between the panel and flanges or between flanges and endplates. When the normalized width-to-thickness ratio exceeds 0.30 for relatively thin panels, cracks grow at the center of the panel.
3) The applicable range of the fatigue relation in Eq. (5.a) is

$$\gamma_a \le 0.11, \; 0.15 \le \frac{h_s}{t_w} \cdot \sqrt{\frac{\tau_u}{\kappa_s \cdot E}} \le 0.30$$

and the subsidiary conditions for panel stiffeners and flange strength are

$$\frac{\gamma_s}{\gamma_s^*} > 3, \quad \frac{A_f \cdot \sigma_{fu}}{\tau_u \cdot t_w \cdot \frac{h}{2}} > 6$$

An effective deformation angle γ_a^* should be used as γ_a in Eq. (9) for a stiffened panel with $0 \le n_r = n_c \le 2$. The effective deformation angle γ_a^* is always larger than the real deformation angle γ_a, because the panel area with welded stiffeners never yields.

4. Fatigue Life Prediction under Earthquake Response

In this section, the expression for the fatigue life prediction of the damper is proposed. Subsequently, the validity of the life prediction expression under severe earthquake is validated through non-stationary amplitude loading tests. Herein, we assume a linear cumulative damage rule (the so-called Palmgren-Miner's law, [8]).

4.1 Fatigue Life Prediction Expression

In Palmgren-Miner's law, the damage factor under multiple-step fatigue testing is written as follows.

$$D_f = \sum_i \frac{N_i}{N_{f,i}} \tag{11.a}$$

where N_i is the number of half-cycles below the *i*th step level loading in a multiple-step fatigue test and $N_{f,i}$ is the number of half-cycles after which the strength has decreased to 0.9 of the maximum value under single-level loading with the *i*th step amplitude.

Palmgren–Miner's law is satisfied without the order of loading amplitudes, and we term N_f in the *k*th half cycle loading as $N_{f,k}$. Then, the damage factor is written as follows.

$$D_f = \sum_k \frac{1}{N_{f,k}} \tag{11.b}$$

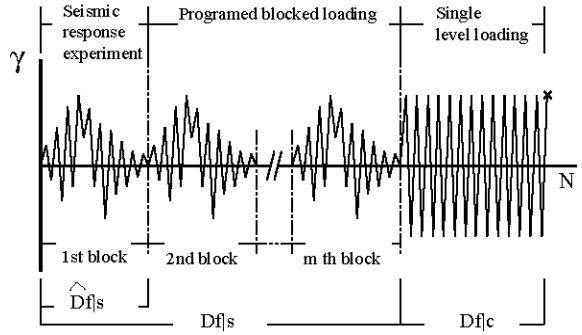

Fig. 6 – Loading Program adopted in Non-Stationary Amplitude Loading Test

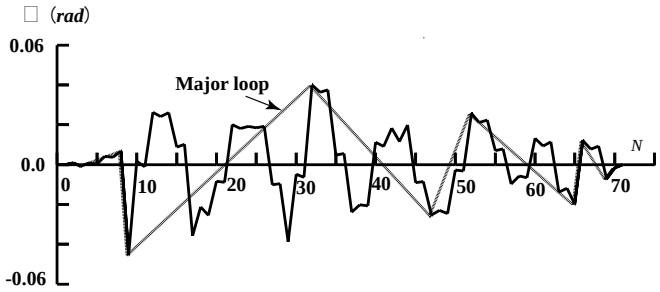

Fig. 7 – Illustration of Shear Deformation Angle Response to Earthquake Ground Motion (21 D.O.F. distributed model, TAFT EW Component)

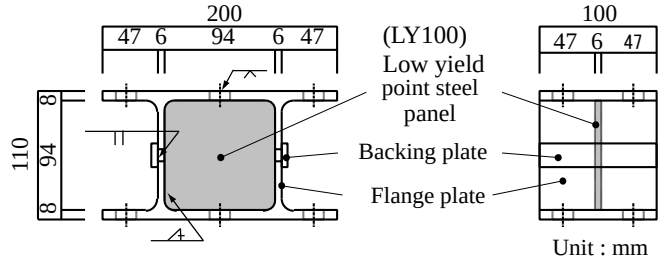

(a) Test Specimen

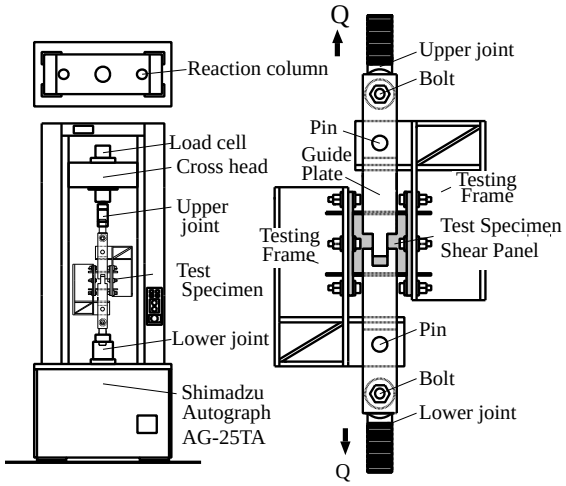

(b) Loading Apparatus

Fig. 8 – Specimen and Loading Apparatus

where $\sum_k$ denotes the summation in accordance with each half cycle.

By substituting Eq. (5.a) into Eq. (11.b), we obtain

$$D_f = 2 \cdot \sum_k \left| \frac{\gamma_{a,k}}{\gamma_f} \right|^C \tag{12}$$

where $\gamma_{a,k}$ is the shear deformation angle amplitude in the *k*th half-cycle. We adopt the rain flow method [32] as a cycle counting procedure under non-stationary amplitude loading, which has the advantage of counting successively from an initial state by using a simple algorithm. Consequently, the fatigue life prediction expression of the damper is obtained as follows:

$$D_f = 1.0 \tag{13.a}$$

where,

$$D_f = 2 \cdot \sum_{kr} \left| \frac{\gamma_{a,kr}}{\gamma_f} \right|^C \tag{13.b}$$

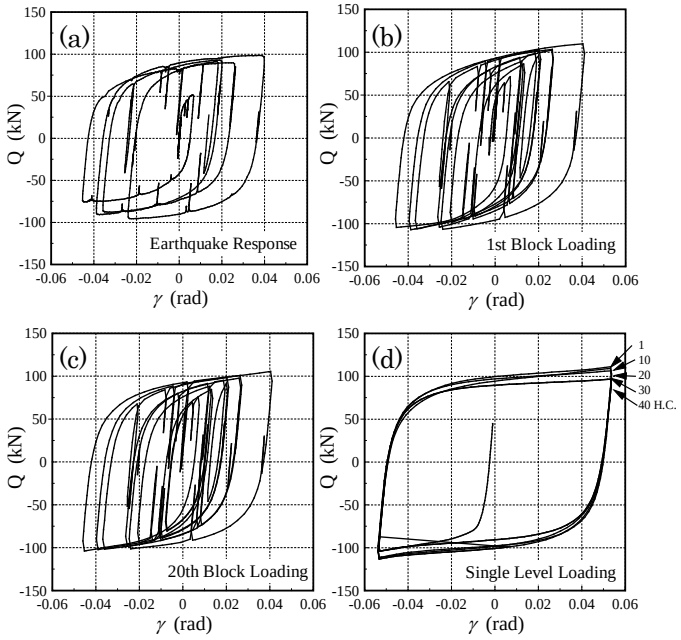

Fig. 9 – Q vs. γ relations in Non-Stationary Amplitude Loading Test
(21 D.O.F. disturbed model, TAFT EW Component)

$\sum_{kr}$ denotes summation over each half cycle, as counted by the rain flow method.

4.2 Validity of Linear Cumulative Damage Rule

To validate the fatigue life prediction expression of Eqs. (13.a,b), non-stationary amplitude fatigue tests using the deformation time history of the S.P.D. in a computer-actuator on-line test [33] are performed.

The adopted deformation time histories are two cases of single-degree-of-freedom (D.O.F.) system responses to the EL CENTRO north/south (NS) and TAFT east/west (EW) components, with maximum ground velocities normalized to 0.35 and 0.30 m/s, respectively, and four cases logging the 7th story responses in two buildings of system with 21 D.O.F., one of which has the optimum dynamic characteristics (Standard model) and the other does not (Disturbed model), to the same earthquake components mentioned above, with the maximum ground velocity normalized by 0.50 m/s. Fig. 6 shows a schematic of the loading program adopted in the test. Fig. 7 shows the deformation angle history of the 21-D.O.F. disturbed model to the TAFT EW component, in the computer-actuator on-line earthquake response tests (Koga et al., 1994). The broken line shows the major loops counted by the rain flow method. The test setup and specimen are shown in Fig. 8. The test specimen is composed of a scaled S.P.D. and L-shaped beams jointed by friction bolts and pin-connected upper and lower screw joints. The scaled S.P.D. is made of a low-yield-point LY100 steel panel surrounded by four cut-tee normal SN400 steel flanges joined by fillet welding. The material properties and dimensions of the test specimen are shown in Table 1 as KLY100-1. To avoid S.P.D. rotation, two guide members are used at the front and rear of the specimen. The loading apparatus is a Shimadzu Autograph AG25-TA, and the specimen is connected through the upper and lower joints to the loading apparatus. During the tests, both compressive and tensile forces act on the S.P.D. through an L-shaped beam, and the S.P.D. is maintained under shear strain identical to that imposed on the specimen installed in the K-braced frame.

The loading measurement is the shear force acting on the S.P.D., Q, which is derived from the load cell installed on the upper cross-head of the apparatus. The displacement measurement is the shear displacement angle of the S.P.D. γ, obtained as the value averaged from the front and rear instruments.

Fig. 9 shows the relationship between load Q and shear deformation angle γ of the damper. In the Fig., (a) is the seismic response, (b) and (c) are programmed block loadings, and (d) is the single-level loading part, respectively.

Table 3 shows the damage factor, where $\hat{D}_f\big|_s$ is the seismic response part, $D_f\big|_s$: is the seismic response and programmed block loading part, $D_f\big|_c$ is the single-level loading part, and D_f is the total damage of all parts until failure. In all specimens, cracks grew in the weld around panel and flanges.

Table 3 – Damage Factors in Non-Stationary Amplitude Loading Tests

D_f			Seismic Loading			Single level loadin		Total
			$\hat{D}_f\big\|_s$	$D_f\big\|_s$	N.O.B	$D_f\big\|_c$	H.C.	D_f
1 D.O.F.		El centro NS	0.0208	0.6448	31	0.3177	31.5	0.9625
		Taft EW	0.0185	0.6845	37	0.2169	21.5	0.9014
21 D.O.F.	Standard	El centro NS	0.0117	0.6552	56	0.1967	19.5	0.8519
	Model	Taft EW	0.0120	0.6480	54	0.2774	27.5	0.9254
	Disturbed	El centro NS	0.0294	0.6174	21	0.3984	39.5	1.0158
	Model	Taft EW	0.0280	0.6160	22	0.2774	27.5	0.8934

N.O.B.: Number of Blocks H.C. : Number of half cycles

From these results, although the strength of the damper under programmed block loading (Fig. 9(b), (c)) is slightly larger than the strength under the seismic response experiment (Fig. 9(a)), the hysteresis loops under the seismic response experiment and under the programmed block loading are almost equal. The total damage factor D_f is ~1.0 for all specimens. Therefore, it is clear that the linear cumulative damage rule is applicable under non-stationary amplitude loading, such as an earthquake response, and the life prediction expression of the damper in Eq. (13.a, b) has sufficient accuracy for practical use. The cumulative damage of the dampers occurring in the responses of the 21 D.O.F. systems with proper structural parameters under severe earthquake ground motion is ~0.0117-0.0294, implying that it is not necessary to replace the damper after a severe earthquake.

5. Conclusions

The applicability of the Manson-Coffin type fatigue relation and the linear cumulative damage rule to the present damper was confirmed through cyclic loading tests. The life prediction expression of the damper was shown and validated by non-stationary amplitude fatigue tests. Furthermore, the cumulative damage values of the damper under severe seismic responses were investigated.

Through these studies, conclusions and remarks from the restricted data are as follows.

1) Under the applied conditions, the Manson-Coffin type fatigue relation with the argument of shear deformation angle sufficiently describes the behavior of the damper under single-level loading.

For a normalized panel width-to-thickness ratio,

$$0.15 \le \frac{h_s}{t_w}\cdot\sqrt{\frac{\tau_u}{\kappa_s\cdot E}} \le 0.30 \quad \text{aspect ratio } 0.5 \le \frac{d_s}{h_s} \le 2.0 \quad \text{and deformation angle } \gamma_a \le 0.11,$$

$$N_f = \frac{1}{2}\cdot\left|\frac{\gamma_a}{\gamma_f}\right|^{-C} \quad \text{where} \quad C = -0.172\cdot\frac{h_s}{t_w}\cdot\sqrt{\frac{\tau_u}{\kappa_s\cdot E}} + 2.74, \quad \gamma_f = -0.449\cdot\frac{h_s}{t_w}\cdot\sqrt{\frac{\tau_u}{\kappa_s\cdot E}} + 0.534$$

2) For $0 \le n_r = n_c \le 2$, which is the number of horizontal and vertical stiffeners, the previous fatigue relation is also applicable to a stiffened panel damper by the use of the effective shear deformation angle. These results were reflected in AIJ design requirements [14].
3) The fatigue life lengthens when the shear deformation angle of the panel is below 0.015 radians. For relatively thick panels, because of shear buckling, cracks grow at the center of the panels even if the normalized width-to-thickness ratio is lower than 0.30. The shear buckling reduces the fatigue life of the panel.
4) A fatigue life prediction is expressed for a relatively thick panel. The expression comprises a rain flow cycle-counting method, a fatigue relation, and a cumulative damage rule. It is sufficiently accurate for engineering use.

5) The damage factor D_f represents the cumulative damage to S.P.Ds. The cumulative damage occurring in the response of the 21-story building with proper structural parameters under severe earthquake ground motion (with about 0.50 m/s in the maximum ground velocity) is ~0.012-0.029, so it is not necessary to replace the damper after a severe earthquake.

Acknowledgements

One study was done as an activity for the subcommittee on Passively Controlled Steel Structures, AIJ (Chair on those days: Kazuhiko Kasai). Fruitful advice and comments were given by members of the subcommittee. These works were supported by JSPS KAKENHI Grant Number 2356087. We would like to express our great thanks for this support.

References

[1] Hjelmstad, K. D. and Popov, E. P., (1983). “Cyclic behavior and design of link beams”, *Journal Structural Engineering, ASCE*, Vol.109, No.10, 2387-2403.

[2] Malley, J. and Popov, E. P. (1984), "Shear Links in Eccentrically Braced Steel Frames", *Journal of Structural Engineering, ASCE*, Vol. 110, No. 9, 2275-2295.

[3] Kasai, K. and Popov, E. G., (1986 a), "General Behavior of WF Steel Shear Link Beams", *Journal of Structural Engineering, ASCE*, Vol.112, No.2, 362-382.

[4] Kasai, K. and Popov, E.P., (1986 b), "Cyclic Buckling Control for Shear Link Beams", *Journal Structural Engineering, ASCE*, Vol.112, No.3, 505-523.

[5] Engelhardt, M. D. and Popov, E. P., (1992). “Experimental performance of long links in eccentrically braced frames.” , *Journal Structural Engineering, ASCE*, Vol.118, No.1, 3067-3088.

[6] IBC, (2004), International Building Code 2004, International Code Council.

[7] Manson S.S., (1966): Thermal Stress and Low Cycle Fatigue. *McGraw Hill*, New York, 125-192.

[8] Miner, M. A. (1945), "Cumulative damage in fatigue", *J. Appl. Mech. Trans. ASME*, 67,159-164.

[9] Japan Society of Material Science (1978), “Handbook of Metal Fatigue”, (in Japanese), Yokendo, 196-212.

[10] Tamai, H., Kondoh, K. and Hanai, M. (1994), “On Low-Cycle-Fatigue Characteristics of Hysteretic Damper and Its Fatigue Life Prediction under Severe Earthquake Ground Motion", (in Japanese), *J. Struct. Constr. Eng., AIJ*, No. 462, 141-150.

[11] Koga, H., Tamai, H., Kondoh, K. and Hanai, M., (1995), "Fatigue Life Prediction of Hysteretic Damper under Severe Earthquake Ground Motion (Part I-II)" , (in Japanese), *Summaries of Technical Papers of Annual Meeting AIJ*, C, III, 389-392, 1995.8.

[12] Architectural Institute of Japan, Subcommittee on Cyclic Loading Effect, (2004), "Cyclic Loading Effect and Fatigue Damage Due To Wind and Earthquake", (in Japanese), Symposium Text.

[13] Tamai, H. (2015), "On Equivalent Shear Buckling Deformation Angle For Shear Panel Damper", (in Japanese), *J. Struct. Constr. Eng., AIJ*, Vol.80,No.707,137-145.

[14] Architectural Institute of Japan (2014): "The Recommended Provision for Seismic Damping Systems Applied to Steel Structures", (in Japanese), Maruzen.

[15] Narihara, H. and Nakagomi T., (2001), "Low Cycle Fatigue Curves of Shear Panel Type Hysteretic Damper made of Low Yield Stress Steel", (in Japanese), *Summaries of Technical Papers of Annual Meeting AIJ*, C, III, 627-628.

[16] Sekine, S., Shinabe, Y. and Takahashi, Y., (1996), "Experimental Study on the Modeling Restoring Force Characteristics of the Shear Resistance Y type Seismic Member, part 3 Low Cycle Fatigue of Low Yield Stress Steel", (in Japanese), *Summaries of Technical Papers of Annual Meeting AIJ*, C, III, 807-808.

[17] Takenaka, H., Chiba, O., Yamaguchi, S., et al., (1998), "Experimental Study on Damping member with Low Yield Strength Steel, Part 3 Results of Single Level Loading Tests ", (in Japanese), *Summaries of Technical Papers of Annual Meeting AIJ*, C, III, 789-790, 1998.9.

[18] Tagami, J., Yoshida, H., Kihara, H., Torii S., et al., (1998),"Dynamic Loading Test of Shear Panel using Low Yield Strength Steel", *Summaries of Technical Papers of Annual Meeting AIJ*, C, III, 777-778.

[19] Kondou, M., Kubota, N., Kobayashi Y., Sugitani H. and Masuo, K., (1999), "Experimental Study on Shear Panel Using Low Yield Strength Steel", (in Japanese), *Summaries of Technical Papers of Annual Meeting AIJ*, C, III, 731-732.

[20] Kanazawa, Y., Ida,T., Tamai, H., et al., (1997), "Influence of Panel Stiffening on Energy Absorbing Capacity of Shear Resisting member Made of SS400 Panel, Part 1,Part 2", (in Japanese), *Summaries of Technical Papers of Annual Meeting AIJ*, C, III, 751-754.

[21] Koga, H., (1996), "Fundamental Study on Mechanical Properties of Hysteretic Damper Installed in Braced Frame", (in Japanese), Master Thesis, Hiroshima Univ.

[22] Hanai, M., Tamai, H., et al., (1993), "Elasto-Plastic Behavior of the Hysteretic Damper using a Low Yield Stress Steel Plate Installed in X-Braced Frame, Part 3 Low Cycle Fatigue Characteristics", (in Japanese), *Summaries of Technical Papers of Annual Meeting AIJ*, C, II,1223-1224.

[23] Izumi, M., Narihara, H. and Yasuda, S., (1996), "Low Cycle Fatigue Test on Shear Yielding Type Low Yield Stress Steel Hysteretic Damper for Response Control, Part 6 Test Results of Width to Thickness Ratio of Web d/tw=90 Series", (in Japanese), *Summaries of Technical Papers of Annual Meeting AIJ*, C, III, 803-804.

[24] Izumi, M., Narihara, H. and Yasuda, S. (1997), "Low Cycle Fatigue Test on Shear Yielding Type Low Yield Stress Steel Hysteretic Damper for Response Control, Part 8 Test Results of Width to Thickness Ratio of Web d/tw=90 , 130 Series", (in Japanese), *Summaries of Technical Papers of Annual Meeting AIJ*, C, III,737-738.

[25] Ryujin, H., Fujinami, K., Yamasaki, T., Tamai, H., et al., (1997), "Very Low Cycle Fatigue Test of Shear Resistance Member Made of SN400B Steel, Part 1, Part 2", (in Japanese), *Summaries of Technical Papers of Annual Meeting AIJ*, C, III, 747-750.

[26] Ueki, T., Katayama, T., Kamura, H., et al., (1999), "Study on Shear Wall Damper Panel using Low Yield Strength Steel, Part1, Part2", (in Japanese), *Summaries of Technical Papers of Annual Meeting AIJ*, C, III, 769-772.

[27] Fujinami, K., Iwaoka, S., Ryujin, H., Tamai, H., et al., (1998), "On the Elasto-Plastic Behavior of Frame with Energy Absorbing K-Brace Made of SN400B Steel, Part1, (in Japanese), Part 2", *Summaries of Technical Papers of Annual Meeting AIJ*, C, III, 831-834.

[28] Tsukatani, H., Koiwa, K., Sawada, N., Kaneko, H. and Suzuki, N., (2001), "Experimental Study on Low Cycle Fatigue Characteristics for Low Yield Strength Steel Shear Panel", (in Japanese), *Summaries of Technical Papers of Annual Meeting AIJ*, C, III,615-616.

[29] Kanazawa, Y., Tamai, H., Kondoh, K., Hanai, M. and Fujinami, K., (2000), "Influence of Inaccurate Stiffening and Panel Shape on energy Absorbing Capacity of Hysteretic Damper Made of SS400 Steel", (in Japanese), *Journal of Constructional Steel*, Vol.8, 117-124.

[30] Ida, T., Kanazawa, Y., Tamai, H., et al., (1997), "Influence of Panel Stiffening on Energy Absorbing Capacity of Shear Resistance member Made of SS400 Steel, part 2", (in Japanese), *Summaries of Technical Papers of Annual Meeting AIJ*, C, III,753-754.

[31] Chusilp, P. and Usami, T., (2002), "New Elastic Stability Formulas for Multiple-Stiffened Shear Panel", *Journal of Structural Engineering, ASCE*, Vol.128, No.6, 833-836.

[32] Endo, T. and Anzai, H., (1981), Refined rain flow algorithm: P/V difference method", (in Japanese), *J. Soc. Mat.Set. Japan*, 30 (328), 89-93.

[33] Koga, H., Kunisue, A., Tamai, H., Kondoh, K. and Hanai, M., (1994), "Application of hysteretic damper to tall building (Part I-III)", (in Japanese), *Summaries of Technical papers of Annual meeting AIJ*, B, 1047-1052.